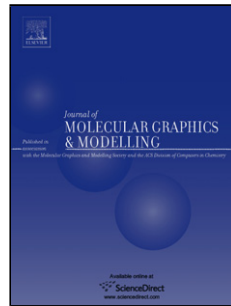


# Accepted Manuscript

Title: Binding of Modulators to Mouse and Human Multidrug Resistance P-glycoprotein. A Computational Study

Author: Gabriel. E. Jara D. Mariano A. Vera Adriana B. Pierini



PII: S1093-3263(13)00156-3

DOI: <http://dx.doi.org/doi:10.1016/j.jmgm.2013.09.001>

Reference: JMG 6332

To appear in: *Journal of Molecular Graphics and Modelling*

Received date: 10-5-2013

Revised date: 8-8-2013

Accepted date: 2-9-2013

Please cite this article as: G.I.E. Jara, D.M.A. Vera, A.B. Pierini, Binding of Modulators to Mouse and Human Multidrug Resistance P-glycoprotein. A Computational Study, *Journal of Molecular Graphics and Modelling* (2013), <http://dx.doi.org/10.1016/j.jmgm.2013.09.001>

This is a PDF file of an unedited manuscript that has been accepted for publication. As a service to our customers we are providing this early version of the manuscript. The manuscript will undergo copyediting, typesetting, and review of the resulting proof before it is published in its final form. Please note that during the production process errors may be discovered which could affect the content, and all legal disclaimers that apply to the journal pertain.

# Binding of Modulators to Mouse and Human Multidrug Resistance P-glycoprotein. A Computational Study

Gabriel. E. Jara,\*[a,c] D. Mariano A. Vera\* [b] and Adriana B. Pierini\* [c]

[a] Present address: INQUIMAE-CONICET. Departamento de Química Inorgánica, Analítica y Química Física, Facultad de Ciencias Exactas y Naturales, Universidad de Buenos Aires, Ciudad Universitaria, Buenos Aires, Argentina.

[b] Departamento de Química. Facultad de Ciencias Exactas y Naturales. Universidad Nacional de Mar del Plata. Funes 3550 – 7600 Mar del Plata, Argentina.

[c] INFQIQC-CONICET. Departamento de Química Orgánica - Facultad de Ciencias Químicas. Universidad Nacional de Córdoba. Edificio de Ciencias II - Ciudad Universitaria – X5000HUA, Córdoba, Argentina.

( \* ) Authors to whom correspondence should be addressed

**Keywords:**

MDR,

P-glycoprotein,

ABC transporters,

Molecular Docking,

Molecular Dynamics,

Free Energies of Binding.

*Abstract.* The human multidrug resistance (MDR) P-glycoprotein (P-gp) mediates the extrusion of chemotherapeutic drugs from cancer cells. Modulators are relevant pharmaceutical targets since they are intended to control or to inhibit its pumping activity. In the present work, a common binding site for Rhodamine 123 and modulators with different modulation activity was found by molecular docking over the crystal structure of the mouse P-gp. The modulators involved a family of compounds, including derivatives of propafenone (3-phenylpropiophenone nucleus) and XR9576 (tariquidar). Our results showed that the relative binding energies estimated by molecular docking were in good correlation with the experimental activities. Preliminary classical molecular dynamics results on selected P-gp/modulator complexes were also performed in order to understand the nature of the prevalent molecular interactions and the possible main molecular features that characterize a modulator. Besides, the results obtained with a human P-gp homology model from the mouse structure are also presented and analyzed. Our observations suggest that the hydrophobicity and molecular flexibility are the main features related to the inhibitory activity. The latter factor would increase the modulator ability to fit the aromatic rings inside the transmembrane domain.

## Introduction

The human multidrug resistance (MDR) P-gp (*mdr1*;ABCB1) transports a wide variety of structurally unrelated compounds outside the cell, using ATP hydrolysis as driving force. The physiological function of P-gp would be to protect the organism from toxins in the diet and the environment. Due to its role, it is highly expressed in intestine, liver and kidney ([1–3]). Its relatively high expression in these organs can affect the pharmacokinetics and the efficacy of several oral drugs, including antineoplastics and antivirals, whereas overexpression of P-gp in some tumor cells seems to be a major obstacle in cancer chemotherapy regimens ([4,5]). Thus, its natural function precludes the therapeutic treatment of many relevant diseases (**Error! Bookmark not defined.**,**Error! Bookmark not defined.**,[6]).

P-gp belongs to the ATP-binding cassette (ABC) superfamily of transporters. Members of this family ubiquitously spread in the three kingdoms and they also play a role in the MDR of pathogen yeasts and bacteria against antimicrobials. Due to its involvement in the treatment of cancer and other human diseases, P-gp is probably the best known of the ABC cassette and thus, it can be considered as a paradigmatic model for this family of transporters ([7–12]). Its 1280 amino acids are arranged as a single chain with two homologous halves having 43% amino acid identity. A linker region of ~60 amino acids connects the two halves of the protein ([13]). Each half has six transmembrane domains (TM) and a hydrophilic domain containing an ATP-binding site, known as nucleotide binding domain (NBD) ([14–18]).

Besides its natural substrates, P-gp can also bind another kind of drugs often called MDR modulators which present the interesting potential of inhibiting or modulating its activity. Since these modulators could control the extrusion of therapeutic cytotoxic drugs, they are hot pharmaceutical targets ([19–26]).

Although there is a considerable amount of physiological and biochemical studies concerning the activity of P-gp (**Error! Bookmark not defined.**-**Error! Bookmark not defined.**) promoting the extrusion of different substrates alone or combined with MDR modulators or inhibitors, the design of effective drugs capable of controlling the MDR activity has two main obstacles. First, from the point of view of Medicinal Chemistry, it is an intrinsically complex task because P-gp recognizes a wide profile of structurally different and unrelated compounds as both, substrates and inhibitors. Thus,

its ability for interacting with such a large number of compounds can be ascribed to either the existence of multiple separated drug-binding sites or a single, large and flexible drug-binding pocket ([27]). Moreover, the absence of a detailed atomic-level description of its structure prevented a rational structure-based design of inhibitors.

In the absence of an X-ray structure of human P-gp, several homology models based on bacterial transporters have been proposed ([28]). Tieleman *et al* ([29]), have built one of such models based on the recent structure of Sav1866 ([30]). Sav1866 is an ABC transporter from *Staphylococcus aureus* with unknown physiological function ([31]), which has been trapped in an outward facing-like conformation (*i.e.* more likely to be the conformation after the ATP hydrolysis and concomitant extrusion of the drug). However, the authors have modeled the protein to yield other two conformations, both of them compatible with a drug binding capable state (**Error! Bookmark not defined.**). Later on, the first crystallographic structure of a mammal P-gp was obtained. This success brings a unique opportunity to evaluate the interactions of new as well as known ([32]) inhibitors into an experimental P-gp structure ([33]). The mouse (*Mus musculus*) P-gp bears a high degree of homology (about 86% amino acid identity) with the human P-gp and it has been convincingly proposed to represent a resting state (nucleotide free), in a fully drug binding competent conformation ([34]). Recently, a crystallographic structure of P-gp from *Caenorhabditis elegans* was obtained with a resolution of 3.4 Å. The protein from *C. elegans* is 46% identical to the human one ([35]). In the present work, we used the experimental mouse P-gp structure because of its much higher homology.

The aim of this work is therefore to clarify the key aspects related to the location of the binding sites and the P-gp/ligand molecular interactions by a multistep computational study. It consists of three steps: 1) Parameterization of ligands; 2) Location of possible binding sites by molecular docking, relating docking energies and experimental activities; 3) Dynamic characterization of the binding mode, energetic decomposition of molecular interactions and identification of the amino acids involved.

Thus, by molecular docking through all the Transmembrane Domain (TMD), we propose the location of the main binding sites for the substrate Rhodamine123, for a family of propafenone-like compounds and for a potent, third generation modulator (mainly focused on XR9576, one of the best modulators known at present). The description of the dynamic of the binding modes and the molecular interactions of these drugs were studied by means of classical molecular dynamics (MD) simulations. Our

analysis along the MD simulations was focused on the conformational changes of the binding site. Upon drug binding we could explain our results by analyzing the rearrangements, mostly due to changes in the packing of the protein side chains, as well as the persistence of the interaction with key residues. In so doing, short MD simulations were performed in order to describe those packing and to avoid any possible unfolding due to the absence of the membrane. Therefore, we consider that the observations here presented would not be widely influenced by its absence. The outcomes from this study could be of help in the rational design of modulators as some key features of the binding in the TMD of this transporter are described; the binding being considered as the first step of the overall process (**Error! Bookmark not defined.**,**Error! Bookmark not defined.**).

## Materials and Methods

### *Parameterization of the Ligand Structures*

The optimized structures of the substrate and modulators were obtained from Quantum Mechanics *ab initio* calculations (QM). The geometries were optimized with the gradient generalized B3LYP ([36,37]) DFT ([38]) functional and gaussian bases 6-31+G(d,p). The properties informed correspond to the lowest energy minima, which were obtained by a conformational search protocol using the semiempirical AM1. The minima were characterized by their harmonic frequencies from the Hessian matrix diagonalization, using the Gaussian 03 package ([39]). The protonation state of the ligands at physiological pH was taken into account, *i.e.* tertiary amines as ammonium single charged cations, aromatic amines as neutrals, Rhodamine 123 as monovalent cation. However, for the case of aliphatic amines the neutral form is proposed to be more likely present due to the very lipophilic transmembrane environment ([40]). In these cases, both neutral and ammonium species were simulated, the former being correlated to the EC50s since their docking energies were just slightly different from those of charged form.

The AMBER force field employed to describe the protein was the ff99sb version ([41]). The general atom force field (GAFF) ([42]) was used to assign the atom types, bond, and nonbond parameters for the non standard residues, *i.e.* substrates and modulators, together with RESP ([43]) partial atomic charges from the electrostatic potential

obtained from the QM calculations at HF/6-31G\*\* level ([44]). All MD simulations were run using AMBER 9 package of programs ([45]). The standard AMBER tools (leap, antechamber, parmchk, parmcal, respin, resp) were used (**Error! Bookmark not defined.**). This type of protocol has been successfully applied for obtaining ligand force field parameters in several studies ([46,47]).

### ***Protein Structure Preparation***

Two structures of the P-gp were used. One of them corresponds to the mouse P-gp experimental structure obtained from ref. **Error! Bookmark not defined.** (PDB code 3G5U; 3.8 Å resolution). The other is our human structure model, built by homology modeling from the mouse P-gp. For both structures, similar preliminary preparation procedures were followed. Thus, partial optimizations for solving local close contacts and strains were performed using PROCHECK ([48]) and the AMBER leap facility. Afterward, 2000 steps of Steepest Descent minimization were applied to the model, holding the backbone atoms constrained. The resulting structure was used for docking and further preparation of the MD runs.

### ***Human P-gp Modeling***

Sequence alignment was done between the mouse PDB sequence (PDB code: 3G5U) and the human P-gp sequence (ID number: p08183) using ClustalW ([49]). Details on the sequence alignment are available as Electronic Supporting Information (SI, Figure S2). Comparative modeling was performed using Modeler 9v7 program ([50]) by selecting the models with the lowest RMSd. Afterwards, the side chains of the whole protein were optimized by 2000 steps of Steepest Descent, holding the backbone atoms constrained. PROCHECK (**Error! Bookmark not defined.**) was used to check the protein structural parameters. The Ramachandran plot of the resulting structure holds more than 84% residues in the core-allowed regions, 15% in allowed regions and less than 0.8% in disallowed ones. The overall backbone RMSd from the experimental structure was 0.77 Å.

A further validation was to compare the distances between C $\alpha$  atoms of the model against the experimental ones. In order to consider a variation of the distances due to the atomic vibration of the backbone, a stochastic dynamics using a G $\ddot{\text{o}}$ -like Hamiltonian was performed with no boundary conditions. In this dynamics we employed a minimalistic representation of the protein in which each amino acid residue is described

by one “bead,” located at the C $\alpha$  position. The Go-like Hamiltonian defines the structure of the homology model as the global energetic minimum. Thus, the C $\alpha$  atoms move around their initial positions (their coordinates in the homology model) along the trajectory obtained ([51]). The stochastic dynamics were run using GROMACS 4.5 package ([52]). The Gromacs topology files were generated with the smog@ctbp webserver ([53]). SMOG generates a structure-based energy function for proteins based on the native contacts (NC), *i.e.* the contacts found in the target structure. As usual in this type of simulations a set of reduced units was used for dynamics variables, e.g. temperature or time (**Error! Bookmark not defined.**, [54,55]). A time step of 0.0005 was employed and the temperature kept at 0.66 with a coupling constant of 1. The simulation was performed for  $4 \times 10^6$  time steps. The cut-off used for van der Waals and coulomb interactions was 20.0 Å, and 4 Å for selecting the NCs. The trajectory was used for computing the average inter-residue distances, which were compared to experimental ones when available.

The structure of the model obtained was deposited as part of the SI (PDB file).

### **Molecular Dynamics**

The protonation states of the histidine residues were assigned by inspection, according to the putative hydrogen bond network wherever it was relevant. The structure of the free enzyme or the enzyme / ligand complex were immersed in a periodic box of about 30000 TIP3P water molecules ( $151 \times 85 \times 86$  Å). Afterwards, MD simulations at constant pressure were carried out for the free enzyme, collecting 4 ns of trajectories after 0.7 ns of equilibration. Prior to these production runs, the systems were relaxed and homogenized following 5000 conjugate gradient optimization steps of the solvent, keeping position restraints on the protein, 25000 optimizations steps of the whole system and a short MD run (100 ps) at constant volume. The system was heated up to 300 K in 0.1 ns and kept at constant temperature and pressure (1 atmosphere) by coupling it to a Berendsen thermostat ([56]). In the equilibrated system, the density slightly fluctuated around 1.019 g/mL. Electrostatic interactions were computed using the Particle Mesh Ewald (PME) method with a cutoff of 10 Å ([57,58]). Bonds involving hydrogen atoms were constrained using the SHAKE algorithm ([59]), this allowing for an integration time step of 0.0015 ps. The trajectories were analyzed using standard AMBER analysis tools. The criteria for analyzing the persistence of H-bonds were set to a maximum length of 3.4 Å (between the heavy atoms) and a maximum angle of 120° (donor-H-

acceptor).

### ***Free Energy Calculations***

The free energies of binding for the protein / modulator complexes were estimated from the equilibrated trajectories using the SIETRAJ ( [60]) algorithm. According to this method, the binding free energy for each snapshot structure is written as the linear combination of the intermolecular electrostatic and van der Waals interactions, polar solvation contribution and the non-polar solvation contribution. The polar solvation contribution is the difference in the reaction field energy between the bound (complex) and the free states (isolated protein and ligand) while the non-polar solvation contribution is estimated from the change in the molecular surface areas upon binding. The intermolecular contribution is calculated with the AMBER force field, while the polar ones are determined by solving the Poisson–Boltzmann equation and the non-polar solvation contributions are proportional to the solvent-excluded surface. The solvation model along with the binding interaction terms were calibrated in a self consistent manner, as described in ref. (**Error! Bookmark not defined.**).

Analysis trajectories were done with AMBER ptraj facility as well as analysis tools of the VMD 1.8.7 package ( [61]). VMD was also used for visualization and rendering of graphics.

### ***Molecular Docking***

The enzyme/modulator or enzyme/substrate complexes were built by docking the ligand using the Autodock 3.0.5 package (**Error! Bookmark not defined.**), which allow us to directly use the RESP charges (from the QM *ab initio* calculations) for the ligands and AMBER charges for the protein, that is the same setup used for the MD simulations. A standard docking procedure was carried out using AMBER charges (including non standard residues, for which the computed RESP charges from QM calculations were used as in the MD setup) within a box holding the whole TMs chamber, with a grid spacing of 0.375 Å. The most stable docked conformations were selected after 4000 genetic algorithm runs (50-100 individuals and up to 100000 generations per run), with 1 individual surviving each generation and standard control options ( [62]). Docking energies and structures informed were subject to cluster analysis with 2.5 Å RMS as criterion.

## Results and Discussion

### ***Homology Structure validation***

The homology model was validated following the procedure by Globisch *et. al.* ([63]), using experimental distances between amino acids obtained by cysteine cross-linking ([64]). In that work, Globisch *et al.* obtained a P-glycoprotein homology model from Sav1866 that represents a conformation closer to the first step of ATP hydrolysis rather than a conformation corresponding to the ATP-bound functional state. However, in this work we focus on the first step, which occurs in P-gp with no nucleotides bound ([65]). More recently, two homology structures of the P-glycoprotein based on the mouse P-gp were published. One of them uses the mouse P-gp bound to QZ59-SSS (PDB code: 3G61) as a template ([66]), and the other is based on a structure free of ligand and nucleotide (PDB code: 3G5U) ([67]).

By comparing the average distance between C $\alpha$  of residues involved in cysteine cross-linking (**Error! Bookmark not defined.**), we observed that the distances between amino acids S222(TM4)-I868(TM10) and S222(TM4)-G872(TM10), I306(TM5)-I868(TM10), I306(TM5)-G872(TM10), I306(TM5)-T945(TM11), I306(TM5)-V982(TM12) and I306(TM5)-G984(TM12) were inside the range distance observed by Loo *et al.*. The calculated inter-residues distances are summarized on Table 1 (see also SI Figures S3 to S5). Nevertheless, the distances observed between L339(TM6)-F942(TM11), L339(TM6)-T945(TM11), L339(TM6)-V982(TM12) and L339(TM6)-A985(TM12), were lower than those reported (**Error! Bookmark not defined.**), with the exception of the pairs L339(TM6)-I868(TM10) and L339(TM6)-G872(TM10) (Table 1). Besides the flexibility of the P-gp and the fact that our model is based on the free mouse P-gp crystal (i.e. the conformation with no substrate bound), these discrepancies could arise from the presence of the cross-linkers itself (used as molecular rulers). Indeed, it is expected that they would inevitably induce some conformational changes, as they have been reported to have certain activity as substrates, as observed in the ATP-ase activity of the Cys-less P-gp (**Error! Bookmark not defined.**,**Error! Bookmark not defined.**).

Our homology model was thus validated by the high sequence identity with mouse P-gp and by structural verifications (see above, Materials and Methods section), as well as against experimental measurements of cysteine cross-linking. These facts allowed us to confirm that our model actually conserves the resting state structure.

### ***Substrates and Modulators***

The substrates and modulators analyzed are presented in Chart 1. In the present study we use Rhodamine 123 as probe substrate. Due to its luminescence properties, the inhibition of the extrusion of this dye has been extensively used to quantify the MDR modulator activity.

A family of the propafenone-type compounds Gp<sub>xx</sub> was used as a set of known modulators. This family has been comprehensively studied by Ecker *et al.* (**Error! Bookmark not defined.**), and its ability to modulate the extrusion of Rhodamine123 has been experimentally determined under the same conditions for the whole family. These authors have also proposed that the H-bond acceptor capacity of the drugs would be one of the most important structural factors which confer MDR modulator activity. Finally, XR9576 (tariquidar), was chosen as a third generation modulator which has one of the highest activities *in vitro* ([68]).

### ***Location of binding sites by Molecular Docking***

The whole TM domains were scanned making no assumptions about the localization of a particular binding site. The primary binding region for Rhodamine was found to be a hydrophobic pocket involving TMs 4, 5 and 6, labeled site P1, which holds important residues of the mouse and the human (the latter in parenthesis) models, for example: S218(S222,TM4), F299(F303,TM5) ([69]), V334(V338,TM6), L335(L339,TM6), F339(F343,TM6), which have already been proposed to play a crucial role for substrate binding on experimental bases (**Error! Bookmark not defined.**,**Error! Bookmark not defined.**,[70,71,72,73]). In the particular case of residue L339, some authors (**Error! Bookmark not defined.**,**Error! Bookmark not defined.**,**Error! Bookmark not defined.**) have suggested that it is involved in the conformational changes connecting the binding to the further ATP hydrolysis rather than being involved in the binding itself. Rhodamine 123 showed its maximum affinity (-10.66 kcal/mol) for this hydrophobic region (Table 2, Figure 1) which is characterized by a relatively negative electrostatic potential (see SI Figure S6). This output results rational for an amphipathic cation such as Rhodamine 123, which bears the positive charge delocalized over its aromatic system. A secondary region which involves hydrophobic and aromatic residues of TM12 was also located. The latter has a docking energy of -9.21 kcal/mol for the cluster with the highest affinity. A detailed view of contacts (M986 among them) ([74]) of one of the poses involving TM12 is available as SI Figure S7. , taking into consideration the differences in docking

energies, the existence of a secondary binding site is not discarded. Thus, the hypothesis of a translocation pathway of the substrates involving an alternate or transient binding site could deserve further experimental and computational analysis.

Best modulators also have their lowest energy conformations in the P1 site (Figure 2), overlapping the regions where the most stable docked conformations of the Rhodamine 123 substrate were found (Figure 2, left panel). This P1 site involves part of TM4, TM5 and mainly TM6. It looks like the apex of an inverted “V”, the “wings” beginning to separate toward the intracellular direction. Although other clusters were found, some of them involving residues in TM12 contacting TM5 through Y303, the preference for the P1 site is evident especially for the best modulators. For example, XR9576, the most potent under study, has almost all the low energy clusters in site P1 (see Figure 3 and S8). In addition, due to its size and flexibility, XR9576 more plenty fills the whole P1 region and even contacts TM12.

All the Gp<sub>xx</sub>'s have the most favorable cluster located at site P1, involving interactions with residues from the TMs 4, 5 and 6 (Figure S9). Many of these residues were involved in  $\pi$ - $\pi$  stacking interactions and other hydrophobic interactions. Some of the residues located in this docking site, (e.g. F303, L304, Y307, Y310 and F343 of the human sequence) have also been reported by Klepsch *et al.* (**Error! Bookmark not defined.**) by molecular docking for compounds of this family. That study has also informed that a quarter of the docked clusters for Gp62 showed a hydrogen bond between the ligand and residue (Y310). However, in the present study, hydrogen bonds involving the amino acids side chains are observed in a small number of clusters and mainly with residue (S218). Furthermore, the hydrogen bond interactions were formed mainly with the backbone. For the protonated form of Gp62 and the other compounds with an aliphatic amine function, the extra proton was generally found either pointing towards the solvent (no specific interaction with residues side chains) or in intramolecular  $\pi$ -cation stacking (analyzing the first clusters of lowest energy).

Gp570, which would be the poorest modulator of the series according to both the experimental EC<sub>50</sub> values (**Error! Bookmark not defined.**) and the calculated docking energy, was found in site P1 (-11.50 kcal/mol, Table 2). This energy is slightly lower but still close to the docking energy found for Rhodamine. All other Gp<sub>xx</sub> docked structures found inside the P1 site are sensitively more stable than that corresponding to Rhodamine. The energies of the most stable docked structures of each Gp<sub>xx</sub> in any site

are summarized on Table 2. The correlation between the affinity for this site and the experimental activities (as Log(EC<sub>50</sub>)) (**Error! Bookmark not defined.**) is presented in Figure 4 for both mouse and human P-gp. As it can be seen in Figure 4, a similar trend was found model for the most stable docked structures in our human P-gp; SI Table S1 summarizes these comparisons.

In contrast to what is expected for a small localized site, the relationship between EC<sub>50</sub> and binding energies is not anticipated to be as simple as a linear correlation. This is mainly due to the complexity of the system and other factors such as the loosing of affinity at the final (outward facing) stage of the extrusion cycle or the lipophilicity required to diffuse through the cellular membrane, among others. Despite these factors, the trend found between the affinity for the P1 site and the experimental activities for most inhibitors is reasonably good ( $R^2=0.5627$  and  $R^2=0.6397$  for mouse and human P-gp, respectively). These results (Figure 4) are consistent with the hypothesis that P1 is the most relevant site for binding. At this point, it is worth to remark that one of the best modulators known up to date (XR9576) has a clearer preference for this site. Moreover, the region between TM4 and 6, involved in the binding, has already been proposed to play a central role in the binding of Rhodamine and other substrates on experimental bases, as discussed above (see also Table 3) (**Error! Bookmark not defined.**,**Error! Bookmark not defined.**,**Error! Bookmark not defined.**,**Error! Bookmark not defined.**,<sup>75]</sup>).

Some of the main interactions responsible for binding in P1 are shown in Figure 2 for Gp240 as representative. The cavity formed by TM4 and 6 has the shape of a hydrophobic pocket and involves hydrophobic contacts with residues proposed to play a key role in the binding of substrates. As confirmed later by MD simulations there are no common H-bond interactions of relevance for the member of this family. In the case of XR9576 and even though this compound has multiple H-bond acceptor groups the most important contacts are strictly hydrophobic (with amino acids bearing non-polar chains) and of  $\pi-\pi$  stacking nature (with aromatic residues).

The results obtained with the homology model built from the mouse experimental structure relates closely to those previously discussed and are available as SI Table S1; the superimposition of the macromolecules together with the ligand lowest docked energy conformation obtained for Gp570, Gp240 and XR9576 are shown as SI Figure S6.

#### *Dynamical description of the interactions P-gp / modulator inside the site P1*

For the mouse P-gp and for the enzyme in complex with both substrate and modulators, short (5ns) MD simulations were carried out in order to introduce the effects of the rearrangement of the inhibitor itself, the surrounding protein residues and part of conformational changes in the backbone, expected to complete relatively quickly. These effects are missing in the static docking approach (protein held fixed) and are relevant to better understand the nature of the interactions with the inhibitors by revealing dynamical features of their binding modes in the complexes. Since P-gp is a membrane protein, this simulation time is expected to be short enough for avoiding protein unfolding symptoms, but long enough for sampling dynamical binding interactions. For the free enzyme, the backbone RMSd was stationary after equilibration, assumed to occur after 700 ps, and remained below 4 Å at the end of the simulation (RMS for the backbone of the whole structure and dissected by domains available as SI Figure S10). The best modulator XR9576 and an intermediate one (in terms of both docking energy and experimental EC50) of the propafenone series, Gp240, were used to simulate the dynamic of the enzyme/modulators system.

The -15.21 kcal/mol docked conformation of P-gp/XR9576 was used as initial structure for running the MD simulation. The simulation was compared to those of the P-gp/Gp240 and P-gp/Rhodamine complexes and to that of the free enzyme.

For the complexes with Gp240 and XR9576, the last 1000 ps of simulation were used to perform an energetic analysis by means of SIETRAJ (**Error! Bookmark not defined.**) for determining the free energy of binding. The values obtained from the dynamics followed the same relative order obtained from the docking studies (Table 2), *i.e.* the binding of XR9576 and Gp240 to the P1 site is around 5 and 2 kcal/mol more stable, respectively, than the binding of Rhodamine. This fact validates the above considerations about the relative affinities of the inhibitors for the site and the relative importance of the different sites, despite the limitations of the docking approach. The energetic decomposition showed that the main contribution to  $\Delta G_{\text{binding}}$  is van der Waals (hydrophobic type), which correlates with the hydrophobicity of the P1 site. In addition, XR9576 is more stable than Gp240 due to this type of interaction. A second main contribution, which also is a hydrophobic type, was the change in non-polar solvation (Figure 5).

The hydrophobic interaction also can be seen in Figure 6 and Table 3, which show that the majority of the residues that interact closer than 4 Å are hydrophobic or aromatic

residues mainly from TMs 4, 5 and 6. A closer view shows that both substrates and inhibitors interact with aromatic residues forming aromatic ring dimers, trimers or tetramers ([76]). The affinity of the ligand increases with the number of aromatic residues that interact with the pocket; this relationship might deserve further studies in order to establish a qualitative (or even a quantitative) correlation.

The MD results showed that the P-gp/XR9576 complex has low hydration in the P1 region as consequence of the persistent hydrophobic interactions involved in the binding. Moreover, the binding of XR9576 reduces the mobility of the whole protein (by comparing the MD trajectories of both the free enzyme and the complex, mainly at the TMs involved in P1). The mobility of the residues in the XR9576-bound and free enzyme are shown as calculated B-factors in Figure 6, together with the residues (mostly aromatic and hydrophobic) in contact and the relative persistence of their interaction.

As shown on Table 3, many of the residues that interacted with either Rhodamine 123, Gp240 or XR9576 were proposed to play an important role in the binding, on experimental basis (Table 3) (**Error! Bookmark not defined.**,**Error! Bookmark not defined.**). Within these residues, S222(TM4), I306(TM5), V338(TM6) and A342(TM6), were common for Rhodamine 123, Gp240 and XR9576.

Besides their relation with experimental studies, a recent theoretical work (**Error! Bookmark not defined.**) has highlighted the relevance of most residues from TM4, 5 and 6 listed on Table 3. In that work, a different docking approach has been applied for members of the same propafenone family. It is interesting to compare the present MD analysis obtained for Gp240 to the detailed clustering analysis performed in that work for the more similar structure (Gp62). Figure 7 summarizes the mobility analysis and the persistency of the contacts analogously to Figure 6 for the case of XR9576. Several residues addressed as more evenly involved in contacts with the propafenone derivative in that work are also those which have very persistent contacts; they being involved more than 50% and in most cases 100% of the simulation time by the present MD analysis. Thus, residues F299(F303), L300(L304), Y307(Y310) from TM 5, A339(A342) and F339(F343) from TM6 and Q712(Q725) from TM7 are involved in the binding by both independent computational analyses.

Most contacts of the initial docked conformation are preserved along the MD trajectory,

but the protein arranges to make more hydrophobic residues to contact to the inhibitor. These rearrangements occur in the first picoseconds of the dynamics, showing a strong relaxation of the binding site. This effect is showed in terms of RMSd of selected residues (Figures S11 and S12 in the SI). Moreover, XR9576 disassembles an H-bond network between residues of the cytoplasmic ends of TM3, 4 and 6 (inter-TM H-bonds). For the case of Gp240, which binds much less tightly than XR9576, the TM12 still approaches the ligand which forms contacts to F979 (F983) and M982 (M986).

The hydrogen acceptors capacity has been suggested as the main characteristic conferring inhibitor activity. However, neither Gp240 nor XR9570, which have 4 and 8 acceptor groups, respectively, are involved in remarkably persistent H-bond interactions. In the binding of Gp240, its OH group (chart 1), acting as H-bond *donor*, binds to the oxygen backbone of A338(A342) with a 55% of persistence (Figure 8). This H-bond acts as an anchor, facilitating the orientation of the Gp240 hydrophobic moieties inside the pocket. XR9576 has more acceptors groups than any Gpxx compound, however, it makes only *one* persistent H-bond as acceptor [with Q721(Q725)]. This analysis suggests that the H-bond acceptor capability would not be the most important structural determinant for the inhibitory activity.

MD simulations were intended to verify the order of stabilities obtained by docking and to better understand the relevance of the different interactions involved in the binding. Despite the fact that the P-gp is a transmembrane protein and longer simulations times would require a lipid bilayer as part of the system, the setup of the protein in an explicit box of solvent has already been used for the P-gp ([84]) and it is expected to recover the local induced fit effects (missing in the docking approach); *e. g.* the rearrangements of the flexible ligand itself together with the side chains of the protein involved in the contacts found by docking. A more realistic description of such motions and further long range conformational changes would be described more appropriately by including the lipid bilayer as part of the simulation. Further long range rearrangements are currently under study using an extended model including the P-gp/XR9576 immersed in a lipid bilayer. These studies are part of work in progress. However and despite the limitations and the difficulties for directly comparing free energies against EC50s (instead of  $K_i$ 's), the free energies of binding obtained from the MD energetic analysis are reasonably in the order of the experimental EC50 for both Gp240 ( $K_i = 0.97 \mu\text{M}$  estimated against 17.61  $\mu\text{M}$  experimental EC50) and XR9576 ( $K_i = 2.1 \text{ nM}$  estimated against 16.3 nM experimental EC50) (**Error! Bookmark not defined.**,<sup>85,86]</sup>).

## Conclusions

The human P-gp model introduced showed a good agreement between the averaged and experimental inter-residue distances measured by cysteine cross-linking. It also was useful for comparing docking simulations between the human and mouse sequences and it would be useful as a structural model for further studies.

Based on our results, the site P1 would be the most important modulator-binding site of P-gp for the inhibitors under study, and it overlaps with the Rhodamine site. Therefore, this description would suggest a competitive scheme for these inhibitors and the substrate Rhodamine 123.

Our results gave a detailed description of the residues involved in what we suggest the main binding pocket, and the regions of the TM's comprised are in agreement with proposals made on experimental bases. Also, we were able to identify some other residues which were still not uncovered by experimental means and that would be involved in the binding with these ligands. The main interactions with the substrates or modulators in the region between TM 4, 5 and 6 are hydrophobic and mainly comprise S222(TM4), I306(TM5), V338(TM6), L339(TM6), A342(TM6) and F343(TM6) (see also Table 3). The binding to this site could reduce the mobility of TM's (especially TM6) which might affect the subsequent ATP-hydrolysis; however, a study which involves a membrane would be necessary for addressing further insights about this issue. By molecular docking, a second site, close to P1 one, was found, which involved TM12 (for example V982). The relevance of this site is not discarded, since in its best docking conformation XR9576 interacts not only with site P1 but also with TM12. The interaction of TM12 with other inhibitors such as Gp240 was also observed by MD. Our studies based on molecular docking and molecular dynamics are in agreement with the proposal of a common drug-binding site (**Error! Bookmark not defined.**). In addition, similar results for some members of the GPxx family were found recently by molecular docking (**Error! Bookmark not defined.**). Even though Gpxx inhibitors could form intramolecular H-bonds (mostly as donors) and their H-bond acceptor capability has been proposed to determine the activity of this family, we consider that this property would not be the most important feature which allows them to bind to the P-gp. Indeed, the hydrophobic interactions were found to have the highest relevance according to our simulations. Also the number of aromatic moieties and the flexibility for arranging them inside the pocket would be considered as relevant structural properties for the inhibitors

under study.

**Acknowledgment.** We gratefully thank Dr. Marcos Villarreal (INFIQC- Universidad Nacional de Córdoba) for helping us in setting up the stochastic dynamics and for discussion of the manuscript. We also gratefully appreciate the suggestions and corrections to our manuscript from Dr. Marcelo Martí (INQUIMAE- Universidad de Buenos Aires).

This work was supported in part by the *Consejo Nacional de Investigaciones Científicas y Tecnológicas* (CONICET), the *Agencia Nacional de Promoción Científica y Técnica* (ANPCYT-Argentina) and the *Secretaría de Ciencia y Técnica* (SECYT) of the *Universidad Nacional de Córdoba*. The INFIQC is jointly sponsored by CONICET and the *Universidad Nacional de Córdoba*. G.E.J. gratefully acknowledges recipient of a fellowship from CONICET. A.B.P and D.M.A.V. are staff members of CONICET.

*Authors declare no conflict of interest.*

**Electronic Supporting Information (SI).**

- 1) PDF file containing: Table S1, which resumes the docking energies for the whole set of compounds docked into the homology model of the human P-gp; Table S2 summarize the free energies of binding estimated by molecular docking for both human and mouse P-gp. All supplementary figures referred within main text as S1 to S12.
- 2) PDB file with the coordinates of the human homology model.

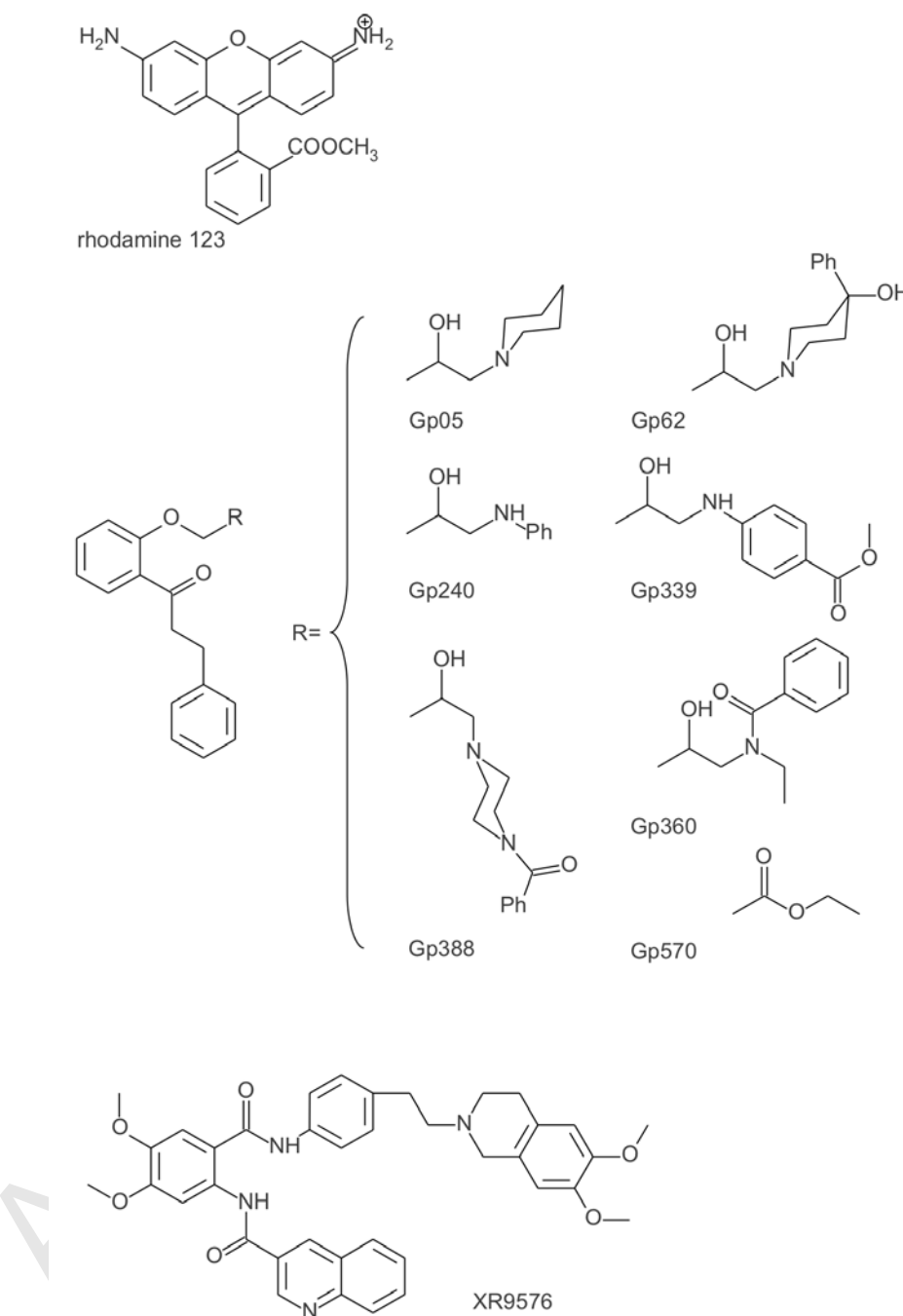


**Chart 1.** Scheme of the substrate (Rhodamine 123) and modulators studied in the present work.

**Table 1.** Comparison between inter-residue distances measured on our homology model *versus* experimental ones.

Amino acids pairs	Homology model average distances (/ Å)	Experimental distances (/ Å) <sup>a</sup>
S222(TM4) - I868(TM10)	30.5	16.8-31.1
S222(TM4) - G872(TM10)	30.7	16.8-31.1
I306(TM5) - I868(TM10)	29.6	20.0-31.1
I306(TM5) - G872(TM10)	28.9	20.0-31.1
I306(TM5) - T945(TM11)	31.0	20.0-31.1
I306(TM5) - V982(TM12)	19.5	20.0-31.1
I306(TM5) - G984(TM12)	22.6	20.0-31.1
L339(TM6) - I868(TM10)	23.1	20.0-31.1
L339(TM6) - G872(TM10)	23.6	20.0-31.1
L339(TM6) - F942(TM11)	24.3	31.1
L339(TM6) - T945(TM11)	22.4	27.3-31.1
L339(TM6) - V982(TM12)	15.4	23.6-31.1
L339(TM6) - A985(TM12)	16.4	27.3-31.1

a) From ref. Error! Bookmark not defined..

**Table 2.** Summary of docking energies and free energy of binding obtained from MD simulations.<sup>a</sup>

Substrate /Inhibitor	Activity	Experimental		Docking energy of the structure		$\Delta G_{\text{binding}}$	Contributions to $\Delta G_{\text{binding}}$ (MD) <sup>f</sup>		
		Log EC <sub>50</sub> <sup>b</sup>	EC <sub>50</sub>	best pose (on P1 in all cases)	best pose P1	vdW	Elec	Non- polar solv.	Polar solv.
Gp05		1.45	0.16	-12.77	-11.88 <sup>c</sup>				
Gp240		17.61	1.25	-12.71	-12.36 <sup>d</sup>	-8.22	-4.64 <sup>g</sup>	-0.26	-0.90
Gp339		4.57	0.66	-13.61	-13.04 <sup>e</sup>				
Gp360		2.57	0.41	-13.59	-13.11 <sup>c</sup>				
Gp388		0.36	-0.44	-14.36	-14.2 <sup>c</sup>				
Gp570		44.45	1.65	-11.50	-11.88 <sup>c</sup>				
Gp62		0.11	-0.96	-13.54	-13.15 <sup>c</sup>				
XR9576									
(Tariquidar)			< -1	-15.21	-13.80 <sup>e</sup>	-11.83	-7.74	-0.76	-1.47
Rhodamine	reference								
123	substrate			-10.66	-9.21 <sup>c</sup>	-7.70	-4.37	0.69	-0.74
									-0.18

<sup>a</sup>) All energies in kcal/mol. Experiments from ref. **Error! Bookmark not defined.**<sup>b</sup>) Experimental EC<sub>50</sub> ( $\mu$ M) for Rhodamine 123 efflux inhibition.<sup>c</sup>) Involved TM12.<sup>d</sup>) Homolog site to site P1, involving TM 10, 11 and 12.<sup>e</sup>) Involved TM 5, 7, 8, 9 and 12<sup>f</sup>) vdw and Elec, are van der Waals and electrostatic interaction, respectively; non-polar solv. and polar solv. are the change of non-polar and polar salvation upon binding, respectively.<sup>g</sup>) The values are scaled by the parameter (0.104758) that SIETRAJ uses to fit  $\Delta G_{\text{binding}}$ .

**Table 3.** Amino acids (A.A) involved in the interaction with the inhibitor within 4 Å for the mouse P-gp. The residues of human P-gp are in parenthesis.

	A.A. Mouse (A.A. Human)	Substrate	Inhibitors		
TM		Rhodamine123	XR9576 (tariquidar)	Gp240	Reference
4	<u>S218(S222)</u>	X	X	X	(Error! Bookmark not defined.,Error ! Bookmark not defined.)
4	P219(P223)	X			
4	L221(L225)	X	X	X	
4	G222(G226)	X	X	X	
4	L223(L227)	X			
4	A225(A229)		X	X	
4	G226(A230)	X		X	
4	A229(A233)			X	
5	N292(N296)		X		
5	I293(I297)		X		
5	M295(I299)		X		
5	G296(G300)		X		
5	F299(F303)		X	X	
5	L300(L304)	X	X	X	
5	<u>I302(I306)</u>	X	X	X	(Error! Bookmark not defined.)
5	Y303(Y307)		X	X	
5	A304(A308)	X			
5	Y306(Y310)	X	X	X	
6	<u>V334(V338)</u>	X	X	X	(Error! Bookmark not defined.)
6	<u>L335(L339)</u>		X		(Error! Bookmark not defined.)

					<b>defined.,Error</b>
					<b>! Bookmark</b>
					<b>not</b>
					<b>defined.,Error</b>
					<b>! Bookmark</b>
					<b>not defined.)</b>
6	G337(G341)	X			
					(Error!
					<b>Bookmark not</b>
					<b>defined.,Error</b>
					<b>! Bookmark</b>
					<b>not defined.)</b>
6	<u>A338(A342)</u>	X	X	X	
					(Error!
					<b>Bookmark not</b>
6	<u>F339(F343)</u>		X	X	<b>defined.)</b>
6	V341(V345)	X		X	
					(Error!
					<b>Bookmark not</b>
6	<b>G342(G346)</b>			X	<b>defined.)</b>
6	S345(S349)			X	
7	N717(N721)		X		
					(Error!
					<b>Bookmark not</b>
7	<u>Q721(Q725)</u>		X	X	<b>defined.)</b>
8	F766(F770)		X		
8	Q769(Q773)		X		
9	A830(A834)		X		
9	F833(T837)		X		
					(Error!
					<b>Bookmark not</b>
					<b>defined.,Error</b>
					<b>! Bookmark</b>
					<b>not</b>
					<b>defined.,Error</b>
					<b>! Bookmark</b>
					<b>not defined.)</b>
12					
	<u>V978(V982)</u>		X		

12	F979(F983)	X	X	(Error! Bookmark not defined.)
12	<u>M982(M986)</u>	X	X	(Error! Bookmark not defined.)
12	<u>Q986(Q990)</u>		X	
12	S989(S993)		X	
12	F990(F994)		X	

---

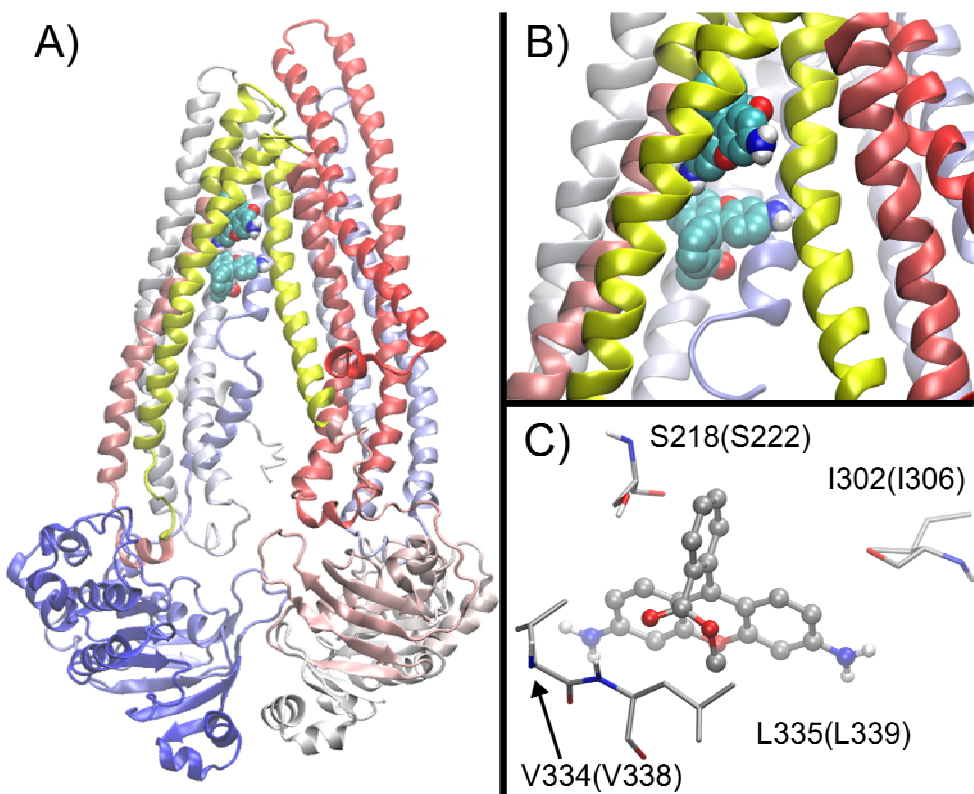


**Figure 1.** A) Docking pose of Rhodamine123 at site P1 (TM 4, 5, 6) and at TM12 backwards (faded) of the mouse P-gp and B) a zoom of the binding region. C) Some of the P-gp residues found in the site P1 for the molecular docking of Rhodamine (within parenthesis human P-gp).

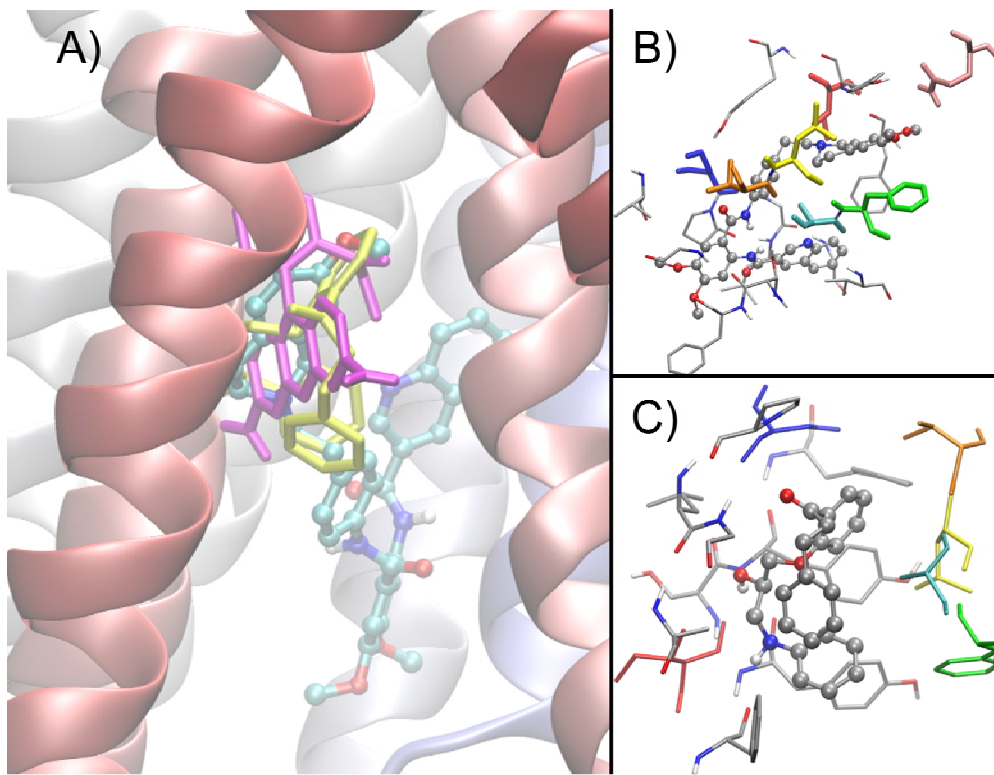


**Figure 2.** A) The docking structure of the low energy conformation of XR9576 (CPK model) superimposed to the substrate Rhodamine123 (yellow) and Gp240 (pink) (left). Contacts of the low energy docked conformation of B) XR9576 and C) Gp240. In B) and C), the amino acids described in bibliography are colored: blue for S218(S222), red for I302(I306), orange for V334(V342), yellow for L335(L339), cyan for A338(A342), green for F339(F343) and pink for V978(V982). The residues of human P-gp are in parenthesis.

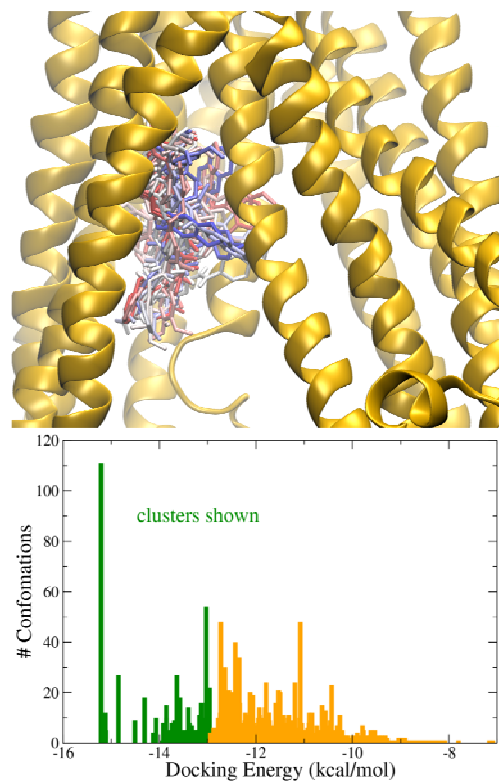


**Figure 3.** Lowest energy conformation of each of the first 25 clusters of lowest energy (green in the histogram of distribution of conformations by cluster *vs.* docking energy) obtained for XR9576 in mouse P-gp. Each of the 25 structures is colored from red to blue (from -16 to -13 kcal/mol docking energy, top image).

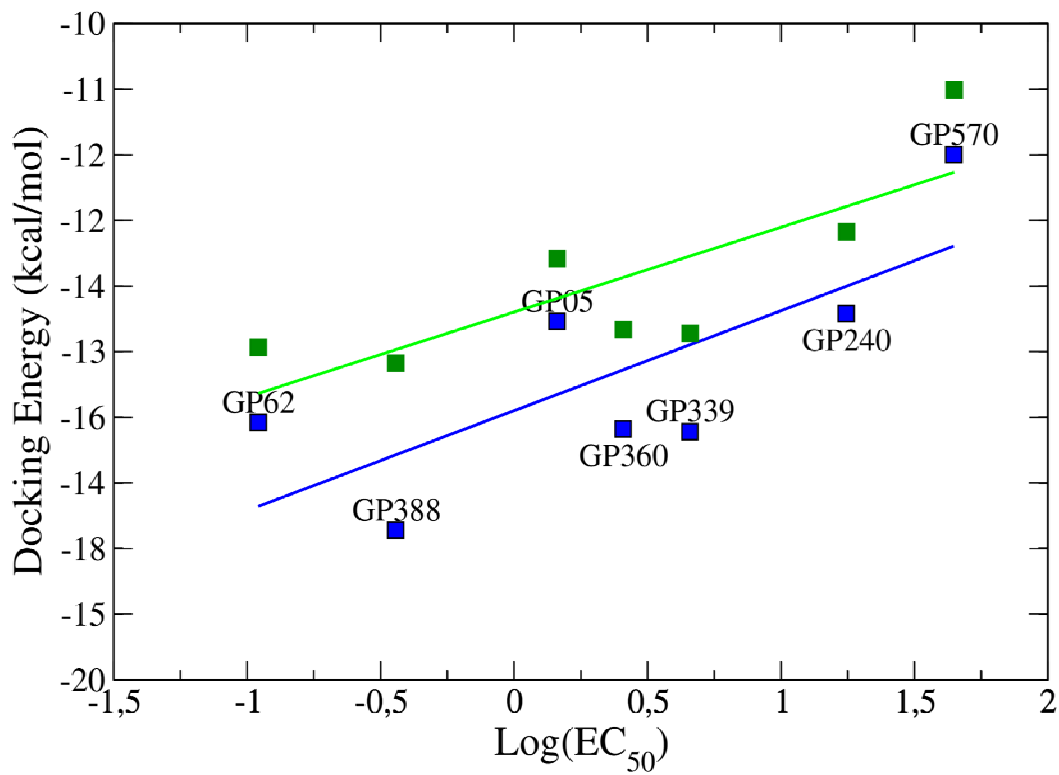


**Figure 4.** Correlation between the docking energy in site P1 and the experimental inhibitory activity against Rhodamine 123 in mouse P-gp (blue) and human P-gp (green).

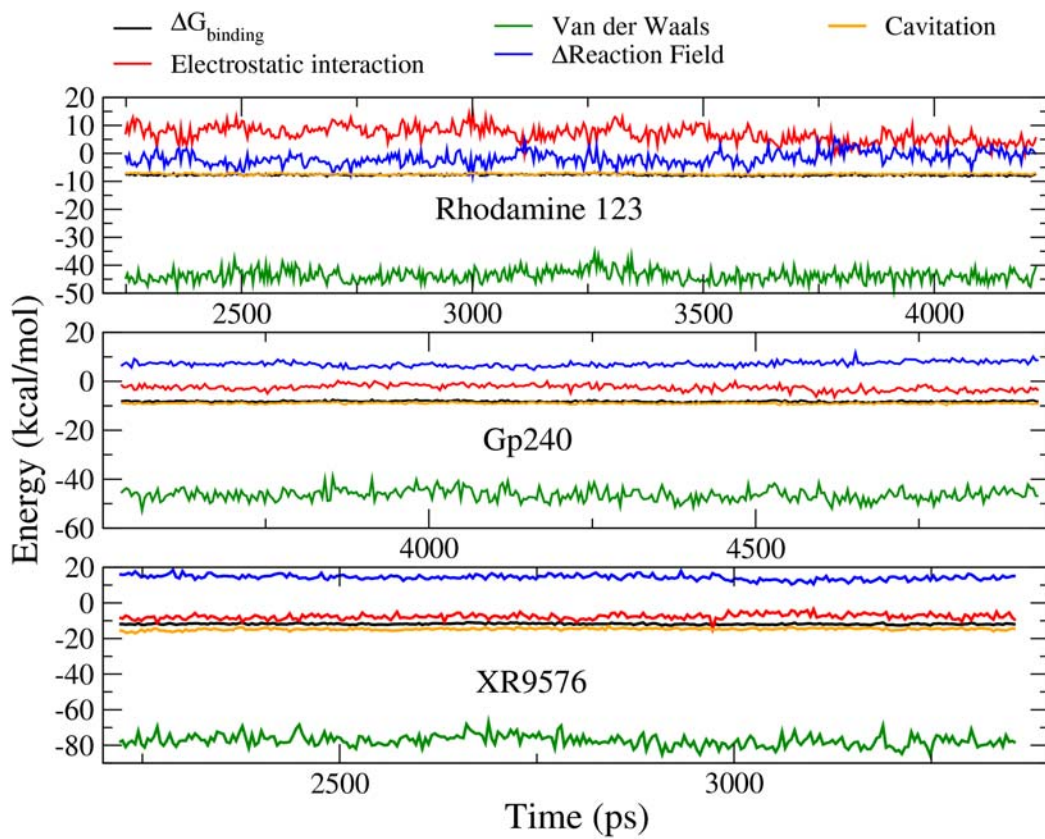


**Figure 5.** Free energy of binding (black lines) as in function of the time for Rhodamine 123, Gp240 and XR9576. Decomposition of binding free energy is showed for van der Waals interactions (green lines), electrostatic interactions (red lines), reaction field (blue lines) and cavitation (orange lines).

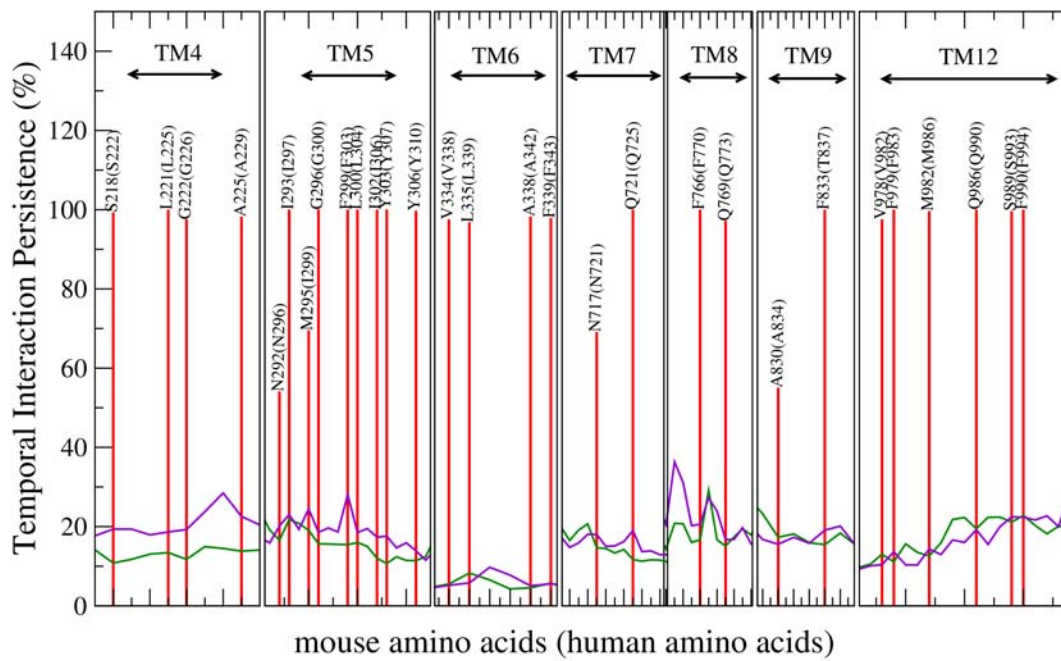


**Figure 6.** % Persistence of amino acids interactions (site P1) along the DM simulation in the XR9576 / mouse P-gp bound complex residues in contact closer than 4 Å are shown as red lines (100% peak intensity indicates that they are in contact to the inhibitor during all frames sampled from 1000 to 4000 ps of the trajectory). B-factors (mobility) of residues in the XR9576-bound and the free enzyme are showed in green and violet lines, respectively. The residues of human P-gp are in parenthesis.

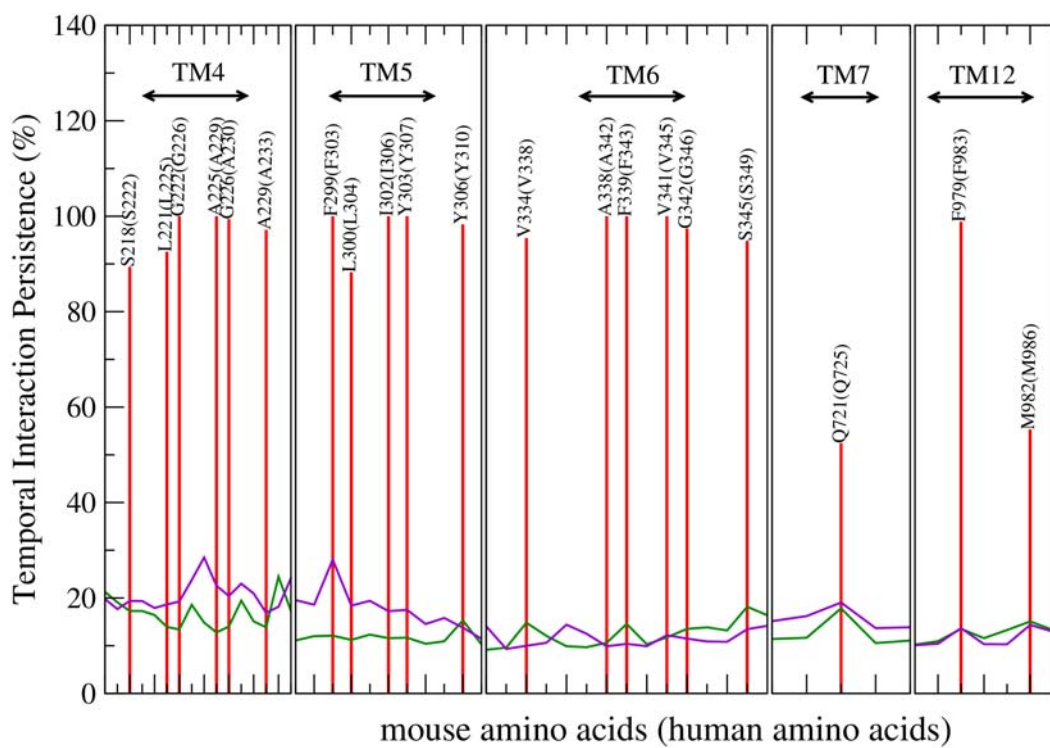


**Figure 7.** % Persistence of amino acids interactions and calculated B-factors for the complex P-gp/Gp240 (same as Figure 6 for XR9576).

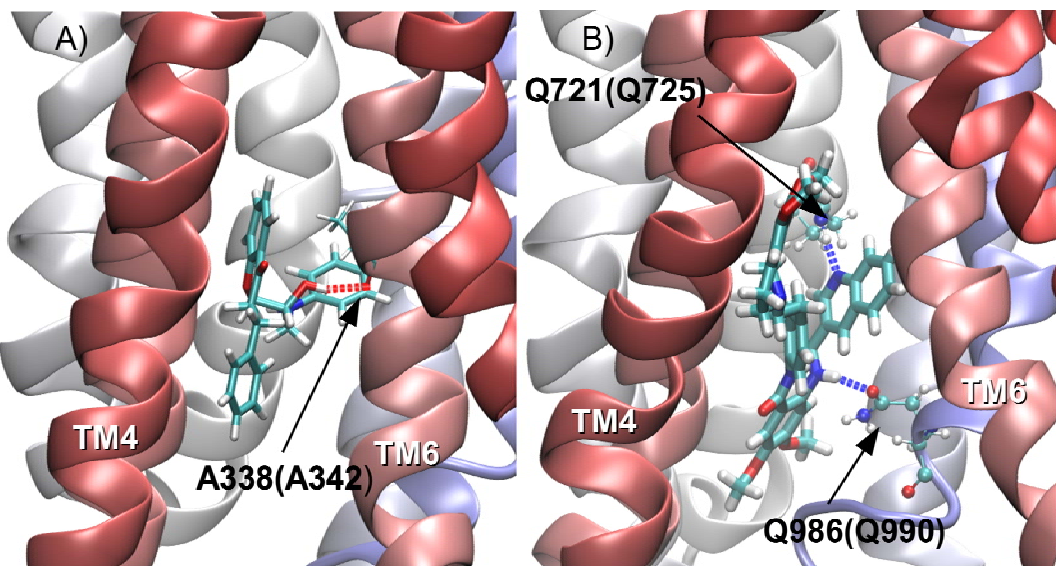


**Figure 8.** Hydrogen bonds formed by Gp240 and XR9576. In both cases the inhibitors acts as H-Bond donors. The H-Bond persistence does not last more than 50% of the complete equilibrated trajectory of the molecular dynamics.

- [1] M.M. Gottesman, T. Fojo, S.E. Bates. Multidrug resistance in cancer: role of ATP-dependent transporters. *Nat Rev Cancer* 2 (2002) 48–58.
- [2] C.A. Hrycyna, Molecular genetic analysis and biochemical characterization of mammalian P-glycoproteins involved in multidrug resistance: *Semin Cell Dev Biol* (2001) 247–256.
- [3] T.W. Loo, D.M. Clarke, Molecular dissection of the human multidrug resistance P-glycoprotein, *Biochem Cell Biol* 77 (1999) 11–23.
- [4] C.G. Lee, M.M. Gottesman, C.O. Cardarelli, M. Ramachandra, K.T. Jeang, S.V. Ambudkar, I. Pastan, S. Dey. HIV-1 Protease Inhibitors Are Substrates for the MDR1 Multidrug Transporter. *Biochemistry* 37 (1998) 3594–3601.
- [5] H. Thomas, H.M. Coley. Overcoming multidrug resistance in cancer: an update on the strategy of inhibiting P-glycoprotein. *Cancer Control* 10 (2003) 159–165.
- [6] K. Paterson, J.A. Ludwig, C. Booth-Genthe, M.M. Gottesman. Targeting multidrug resistance in cancer. *Nat Rev Drug Discov* 5 (2006) 219-234.
- [7] C.F. Higgins. ABC transporters: from microorganisms to man. *Annu. Rev. Cell Biol* 8 (1992) 67-113.
- [8] M. Dean. The human ATP-binding cassette (ABC) transporter superfamily. *Genome Res* 11 (2001) 1156–1166.
- [9] A.H. Schinkel, J.W. Jonker. Mammalian drug efflux transporters of the ATP binding cassette (ABC) family: an overview. *Adv Drug Deliv Rev* 55 (2003) 3–29.
- [10] K.J. Linton. Structure and Function of ABC Transporters. *Physiology* 22 (2007) 122-130.
- [11] J. Lubelski, W.N. Konings, A.J.M. Driessens. Distribution and Physiology of ABC-Type Transporters Contributing to Multidrug Resistance in Bacteria. *Microbiol Mol Biol Rev*. 71 (2007) 463-476.
- [12] F.J. Sharom. ABC multidrug transporters: structure, function and role in chemoresistance. *Pharmacogenomics* 9 (2008) 105-127.
- [13] C.J. Chen, J.E. Chin, K. Ueda, D.P. Clark, I. Pastan, M.M. Gottesman, I.B. Roninson. Internal duplication and homology with bacterial transport proteins in the mdr1 (P-glycoprotein) gene from multidrug-resistant human cells. *Cell*, 47 (1986)

381–389.

- [14] T.W. Loo, D.M. Clarke. Membrane Topology of a Cysteine-less Mutant of Human P-glycoprotein. *J Biol Chem* 270 (1995) 843–848.
- [15] C. Kast, V. Canfield, V. Levenson, P. Gross. Transmembrane Organization of Mouse P-glycoprotein Determined by Epitope Insertion and Immunofluorescence. *J Biol Chem* 271 (1996) 9240–9248.
- [16] T.W. Loo, D.M. Clarke. The Minimum Functional Unit of Human P-glycoprotein Appears to be a Monomer. *J Biol Chem* 271 (1996) 27488–27492.
- [17] T.W. Loo, D.M. Clarke. Reconstitution of drug-stimulated ATPase activity following co-expression of each half of human P-glycoprotein as separate polypeptides. *J Biol Chem* 269 (1994) 7750–7755.
- [18] T.W. Loo, D.M. Clarke. The Transmembrane Domains of the Human Multidrug Resistance P-glycoprotein Are Sufficient to Mediate Drug Binding and Trafficking to the Cell Surface. *J Biol Chem* 274 (1999) 24759–24765.
- [19] N. Dodic, B. Dumaitre, M. Daugan, P. Pianetti. Synthesis and Activity against Multidrug Resistance in Chinese Hamster Ovary Cells of New Acridone-4-carboxamides. *J Med Chem* 38 (1995) 2418-2426.
- [20] A. Dhainaut, G. Regnier, A. Tizot, S. Leonce, N. Guilbaud, N. Kraus-Berthier, G. Atassi. New Purines and Purine Analogs as Modulators of Multidrug Resistance. *J Med Chem* 29 (1996) 4099-4108.
- [21] G. Ecker, P. Chiba, M. Hitzler, D. Schmid, K. Visser, H.P. Cordes, et al., Structure-activity relationship studies on benzofuran analogs of propafenone-type modulators of tumor cell multidrug resistance., *J Med Chem* 39 (1996) 4767–4774.
- [22] I. Pajeva, M. Wiese. Molecular Modeling of Phenothiazines and Related Drugs As Multidrug Resistance Modifiers: A Comparative Molecular Field Analysis Study. *J Med Chem* 41 (1998) 1815-1826.
- [23] D.J. Gruol, M.N. King, M.E. Kuehne, Evidence for the locations of distinct steroid and Vinca alkaloid interaction domains within the murine mdr1b P-glycoprotein., *Mol Pharm* 62 (2002) 1238–1248.
- [24] T.W. Loo, M.C. Bartlett, D.M. Clarke. Methanethiosulfonate derivatives of rhodamine and verapamil activate human P-glycoprotein at different sites. The

- Journal of Biological Chemistry. 278 (2003) 50136–50141.
- [25] C. Martin, G. Berridge, C.F. Higgins, P. Mistry, P. Charlton, R. Callaghan. Communication between multiple drug binding sites on P-glycoprotein., Molecular Pharmacology. 58 (2000) 624–632.
- [26] A. Garrigues, N. Loiseau, M. Delaforge, J. Ferté, M. Garrigos, F.O. André, S. Orlowski. Characterization of Two Pharmacophores on the Multidrug Transporter P-Glycoprotein. Mol Pharm 62 (2002) 1288-1299.
- [27] F.J. Sharom. Shedding light on drug transport: structure and function of the P-glycoprotein multidrug transporter (ABCB1). Chem Cell Biol 84 (2006) 979-992.
- [28] See for example: D.R. Stenham, J.D. Campbell, M.S.P. Sansom, C.F. Higgins, I.D. Kerr, K.J. Linton, An atomic detail model for the human ATP binding cassette transporter P-glycoprotein derived from disulfide cross-linking and homology modeling., FASEB J 17 (2003) 2287–2289.
- [29] M.L. O'Mara, D.P. Tielemans, P-glycoprotein models of the apo and ATP-bound states based on homology with Sav1866 and MalK., FEBS Lett 581 (2007) 4217–4222.
- [30] R.J.P. Dawson, K.P. Locher, Structure of a bacterial multidrug ABC transporter., Nature. 443 (2006) 180–185.
- [31] Despite its natural substrate profile, it has been proved that Sav1866 is capable of translocate typical human P-gp substrate, as well as being inhibited by verapamil, also a known P-gp modulator. See : S. Velamakanni, Y. Yao, D. Gutmann, Multidrug Transport by the ABC Transporter Sav1866 from *Staphylococcus aureus*, Biochem 47 (2008) 9300–9308.
- [32] G.F. Ecker, M. Huber, D. Schmid, P. Chiba. The importance of a nitrogen atom in modulators of multidrug resistance., Mol Pharmacol 56 (1999) 791–796.
- [33] S.G. Aller, J. Yu, A. Ward, Y. Weng, S. Chittaboina, R. Zhuo, et al., Structure of P-glycoprotein reveals a molecular basis for poly-specific drug binding., Science 323 (2009) 1718–1722.
- [34] D.A.P. Gutmann, A. Ward, I.L. Urbatsch, G. Chang, H.W. van Veen. Understanding polyspecificity of multidrug ABC transporters: closing in on the gaps in ABCB1. Trends Biochem Sci 35 (2010) 36–42.

- [35] M.S. Jin, M.L. Oldham, Q. Zhang, J. Chen Crystal structure of the multidrug transporter P-glycoprotein from *Caenorhabditis elegans*. *Nature* 490 (2012) 566–569.
- [36] A.D. Becke. Density-functional exchange-energy approximation with correct asymptotic behavior. *Phys Rev A* 38 (1988) 3098–3100.
- [37] C. Lee, W. Yang, R.G. Parr. Development of the Colle-Salvetti correlation-energy formula into a functional of the electron density. *Phys Rev B* 37 (1988) 785–789.
- [38] W. Kohn, I. Sham. Self-Consistent Equations Including Exchange and Correlation Effects. *J Phys Rev* 140 (1965) A1133-A1138.
- [39] Gaussian 03, Revision B.04, 2003, Gaussian, Inc., Pittsburgh, PA.  
<http://www.gaussian.com>.
- [40] G. S. Retzingerl, L. Cohen, S. H. Lau, F. J. Kézdy. Ionization and Surface Properties of Verapamil and Several Verapamil Analogues. *J Pharm Sci* 75 (1986) 976-982.
- [41] D.A. Pearlman, D.A. Case, J.W. Caldwell, W.S. Ross, T.E. Cheatham, S. Debolt, D. Ferguson, G. Seibel, P. Kollman. Amber, a package of computer programs for applying molecular mechanics, normal mode analysis, molecular dynamics and free energy calculations to simulate the structural and energetic properties of molecules. *Comput Phys Commun* 91 (1995) 1-41.
- [42] J. Wang M. Romain, J.W. Caldwell, P.A. Kollman, D.A. Case, Development and testing of a general Amber force field. *J. Comput. Chem.* 25 (2004) 1157-1174.
- [43] C.I. Bayly, P. Cieplak, W.D. Cornell, P.A. Kollman, P.A The procedure of the determination of RESP charges. *J Phys Chem* 97 (1993) 10269–10275.
- [44] D. Suarez, K.M. Jr. Merz. Molecular dynamics simulations of the mononuclear zinc- $\beta$ -lactamase from *Bacillus Cereus*. *J Am Chem Soc* 123 (2001) 3759-3770.
- [45] AMBER 9, 2009, University of California, San Francisco, CA.
- [46] D.M. Moreno, M.A. Martí, P.M. De Biase, D.A. Estrín, V. Demicheli, R. Redi, L. Boechi. Exploring the molecular basis of human manganese superoxide dismutase inactivation mediated by tyrosine 34 nitration. *Arch Biochem and Biophys* 507 (2011) 304-309.

- [47] T.C. Ramalho, T.C.C. França, W.A. Cortopassi, A.S. Gonçalves, A.W.S. Da Silva E.F.F. Da Cunha. Topology and dynamics of the interaction between 5-nitroimidazole radiosensitizers and duplex DNA studied by a combination of docking, molecular dynamic simulations and NMR spectroscopy., *J Mol Struct* 992 (2011) 65-71.
- [48] R.A. Laskowski, M.W. MacArthur, D.S. Moss, J.M. Thornton. PROCHECK: a program to check the stereochemical quality of protein structures. *J. App. Cryst.* 26, (1993) 283-291.
- [49] J.D. Thompson, D.G. Higgins, T.J. Gibson. CLUSTALW. Improving the sensitivity of progressive multiple sequence alignment through sequence weighting, position-specific gap penalties and weight matrix choice. *Nucleic Acids Res* 22 (1994) 4673-4680.
- [50] N. Eswar, M.A. Marti-Renom, B. Webb, M.S. Madhusudhan, D. Eramian, M. Shen, U. Pieper, A. Sali. Comparative Protein Structure Modeling With MODELLER. *Current Protocols in Bioinformatics, Supplement 15* (2006) 5.6.1-5.6.30.
- [51] A. Clementi, H. Nymeyer, J.N. Onuchic, Topological and energetic factors: what determines the structural details of the transition state ensemble and “en-route” intermediates for protein folding? An investigation for small globular proteins. *J. Mol. Biol.* **298** (2000) 937–953
- [52] B. Hess, C. Kutzner, D. van der Spoel, E. Lindahl, GROMACS 4: Algorithms for Highly Efficient, Load-Balanced, and Scalable Molecular. *J. Chem. Theory Comput.* 4 (2008) 435-447.
- [53] J.K. Noel, P.C. Whitford, K.Y. Sanbonmatsu, J.N. Onuchic. SMOG@ctbp: simplified deployment of structure-based models in GROMACS. *Nucleic Acids Res.* 38 (2010) W657–W661.
- [54] In this context, for a couple of beads of mass  $M$  connected by a distance  $\sigma$  which have an interaction energy of  $-\varepsilon$  in the native state, the dimensionless time  $t_r$  is related to the real time  $t$  by the expression:
- [55] F.K. von Gottberg, K.A. Smith, T.A. Hatton, Stochastic dynamics simulation of surfactant self-assembly. *J. Chem. Phys.* 106 (1997) 9850.
- [56] H.J.C. Berendsen, J.P.M. Postma, W.F. Gunsteren, A. Di Nola. J.R. Haak, J.R.

- Molecular dynamics with coupling to an external bath. *J Chem Phys* 81 (1984) 3684–3690.
- [57] T. Darden, D. York, L.G. Pedersen. Particle mesh Ewald: An  $N \cdot \log(N)$  method for Ewald sums in large systems. *J Chem Phys* 98 (1983) 10089–10094.
- [58] U. Essman, L. Perera, M.L. Berkowitz, T. Darden, H. Lee, L. Pedersen. A smooth particle mesh Ewald method. *J Chem Phys* 103 (1995) 8577–8593.
- [59] J.P. Ryckaert, G. Cicotti, H.J.D.C. Berendsen. Numerical Integration of the Cartesian Equations of Motion of a System with Constraints: Molecular Dynamics of *n*-Alkanes. *J Comput Phys* 23 (1997) 327–341.
- [60] M. Naïm, S. Bhat, K.N. Rankin, S. Dennis, S.F. Chowdhury, I. Siddiqi, et al., Solvated interaction energy (SIE) for scoring protein-ligand binding affinities. 1. Exploring the parameter space., *J Chem Inf Model* 47 (2007) 122–133.
- [61] H. Humphrey, A. Dalke, K. Schulten. VMD - Visual Molecular Dynamics. *J Molec Graph* 14 (1996) 33-38.
- [62] G.M. Morris, D.S. Goodsell, R.S. Halliday, R. Huey, W.E. Hart, R.K. Belew, A.J. Olson. Automated docking using a Lamarckian genetic algorithm and an empirical binding free energy function. *J. Comp Chem* 19 (1998) 1639-1662.
- [63] C. Globisch, I.K. Pajeva, M. Wiese, Identification of putative binding sites of P-glycoprotein based on its homology model., *ChemMedChem*. 3 (2008) 280–295.
- [64] T.W. Loo, D.M. Clarke, Determining the dimensions of the drug-binding domain of human P-glycoprotein using thiol cross-linking compounds as molecular rulers., *J Biol Chem* 276 (2001) 36877–36880.
- [65] T.W. Loo, D.M. Clarke, Vanadate trapping of nucleotide at the ATP-binding sites of human multidrug resistance P-glycoprotein exposes different residues to the drug-binding site., *Proc Nat Acad Sci USA* 99 (2002) 3511–3516.
- [66] Á. Tarcsey, G. Keserü. Homology modeling and binding site assessment of human P-glycoprotein. *Fut Med Chem* 3 (2011) 297-307.
- [67] F. Klepsch, P. Chiba, G.F. Ecker, Exhaustive sampling of docking poses reveals binding hypotheses for propafenone type inhibitors of p-glycoprotein., *PLoS Comput Biol* 7 (2011) e1002036.
- [68] C. Globisch, I.K. Pajeva, M. Wiese. Structure-activity relationships of a series

of tariquidar analogs as multidrug resistance modulators., *Bioorg Med Chem.* 14 (2006) 1588–1598.

[69] The residues discussed are conserved between *H. sapiens* and *M. musculus* species. Since the sequences are aligned, the residue numbers correspond to the human P-gp unless explicitly indicated.

[70] Y. Taguchi, M. Morishima, T. Komano, K. Ueda. Amino acid substitutions in the first transmembrane domain (TM1) of P-glycoprotein that alter substrate specificity. *FEBS Lett* 413 (1997) 142.

[71] T.W. Loo, D.M. Clarke, Mutations to amino acids located in predicted transmembrane segment 6 (TM6) modulate the activity and substrate specificity of human P-glycoprotein., *Biochem* 33 (1994) 14049–14057.

[72] T.W. Loo, D.M. Clarke, Identification of residues in the drug-binding site of human P-glycoprotein using a thiol-reactive substrate. *J Biol Chem* 272 (1997) 31945–31948.

[73] A. Rothnie, J. Storm, R. McMahon, A. Taylor, I.D. Kerr, R. Callaghan. The coupling mechanism of P-glycoprotein involves residue L339 in the sixth membrane spanning segment. *FEBS Lett* 579 (2005) 3984–3990.

[74] T.W. Loo, D.M. Clarke. Drug-stimulated ATPase activity of human P-glycoprotein requires movement between transmembrane segments 6 and 12, *J Biol Chem* 272 (1997) 20986–20989.

[75] T.W. Loo, M.C. Bartlett, D.M. Clarke. Val133 and Cys137 in transmembrane segment 2 are close to Arg935 and Gly939 in transmembrane segment 11 of human P-glycoprotein. *J Biol Chem* 279 (2004) 18232–18238.

[76] E. Lanzarotti, R.R. Biekofsky, D.A. Estrín, M.A. Martí, A.G Turjanski. Aromatic-aromatic interactions in proteins: beyond the dimmer., *J Chem Inf Model* 51 (2011) 1623–1633.

[77] T.W. Loo, M.C. Bartlett, D.M. Clarke, Suppressor mutations in the transmembrane segments of P-glycoprotein promote maturation of processing mutants and disrupt a subset of drug-binding sites. *J Biol Chem* 282 (2007) 32043–32052.

[78] T.W. Loo, D.M. Clarke. Defining the drug-binding site in the human multidrug

- resistance P-glycoprotein using a methanethiosulfonate analog of verapamil, MTS-verapamil. *J Biol Chem* 276 (2001) 14972–14979.
- [79] T.W. Loo, D.M. Clarke, Identification of residues within the drug-binding domain of the human multidrug resistance P-glycoprotein by cysteine-scanning mutagenesis and reaction with dibromobimane. *J Biol Chem* 275 (2000) 39272–39278.
- [80] G.F. Ecker, E. Csaszar, S. Kopp, B. Plagens, W. Holzer, W. Ernst, P. Chiba. Identification of ligand-binding regions of P-glycoprotein by activated-pharmacophore photoaffinity labeling and matrix-assisted laser desorption/ionization-time-of-flight mass spectrometry., *Mol Pharmacol* 61 (2002) 637–648.
- [81] J. Storm, M.L. O'Mara, E.H. Crowley, J. Peall, D.P. Tielemans, I.D. Kerr, R. Callaghan. Residue G346 in transmembrane segment six is involved in inter-domain communication in P-glycoprotein. *Biochem* 46 (2007) 9899–9910.
- [82] T.W. Loo, M.C. Bartlett, D.M. Clarke, Transmembrane segment 7 of human P-glycoprotein forms part of the drug-binding pocket *Biochem J* 399 (2006) 351–359.
- [83] T.W. Loo, D.M. Clarke. Mutational analysis of ABC proteins., *Arch Biochem Biophys* 476 (2008) 51–64.
- [84] A. Sakurai, Y. Onishi, H. Hirano, M. Seigneuret, K. Obanayama, G. Kim, E.L. Liew, T. Sakaeda, K. Yoshiura, K. Niikawa, M. Sakurai, T. Ishikawa. Quantitative Structure-Activity Relationship Analysis and Molecular Dynamics Simulation To Functionally Validate Nonsynonymous Polymorphisms of Human ABC Transporter ABCB1 (P-Glycoprotein/MDR1). *Biochem* 46 (2007) 7678-7693.
- [85] M. Roe, A. Folkes, P. Ashworth, J. Brumwell, L. Chima, S. Hunjan, I. Pretswell, W. Dangerfield, H. Ryder, P. Charlton. Reversal of P-glycoprotein mediated multidrug resistance by novel anthranilamide derivatives. *Bioorg Med Chem Lett.* 9 (1999) 595–600.
- [86] The compared values of EC50 were measured with different substrates, Rhodamine 123 for Gp240 and vinblastine for XR9576.

### Highlights

A main binding site, common to both substrates and modulators, is proposed.

New residues involved in the binding are proposed.

The main component of the free energy of binding is the van der Waals interactions.

Flexibility would be a modulator feature in order to fit its lipophilic moieties.

Capability to fit the lipophilic moieties would be a main feature of a modulator.

